ELSEVIER

Contents lists available at ScienceDirect

Composites Part B

journal homepage: www.elsevier.com/locate/compositesb



Multifunctional primer film made from percolation enhanced CNT/Epoxy nanocomposite and ultrathin CNT network



Hyehee ${\rm Kim}^{\,a,1}$, Sen Gao a,1 , Sanghyun Hong b , Pyoung-Chan Lee c , Young Lae ${\rm Kim}^{\,d}$, Jin Uk Ha c , Sun Kyoung Jeoung c , Yung Joon Jung a,*

- ^a Department of Mechanical and Industrial Engineering, Northeastern University, Boston, MA, 02115, USA
- ^b Gasan R&D Center, LG Electronics, 51, Gasan digital 1-ro, Geumcheon-gu, Seoul, 08592, South Korea
- Materials Technology R&D Division, Korea Automotive Technology Institute, 303 Pungse-ro, Pungse-myeon, Dongnam-gu, Cheonan-si, Chungnam, 31214, South Korea
- d Department of Electronic Engineering, Gangneung-Wonju National University, 7 Jukheon-gil, Gangneung, Gangwon-Do, 25457, South Korea

ARTICLE INFO

Keywords: Polyphenylene sulfide Carbon nanotube Epoxy composite primer Electromagnetic interference shielding

ABSTRACT

Here we demonstrate a high performance multifunctional thin primer film made from sandwich structured ultrathin carbon nanotube (CNT) networks and carbon nanotube-epoxy nanocomposite. For this, percolation enhanced CNT-epoxy nanocomposites were fabricated by mixing CNTs with two extremely different length/diameter aspect ratios followed by a unique convective coating process assembling SWNTs into ultrathin, uniform and large-scale film on hydrophobic CNT-epoxy substrates without any pretreatment of the surface. This multifunctional-sandwiched film exhibits relatively low surface roughness, high conductivities, excellent adherence to both polymers and metals, and tunable high EMI-shielding effectiveness of 32.54 dB in the range of 8.2–12.4 GHz (X-band). These results open the pathway to design multifunctional primer thin films that can be used for fabricating hybrid thermal management systems, EMI shielding film and structurally integrated sensors.

1. Introduction

High performance polymers have attracted significant interests due to their lightweight and enhanced physical properties replacing the use of metals in automobile and aerospace industries [1,2]. Particularly the advancement of electric vehicles requires lightweight materials with a variety of functions such as highly effective thermal management in the battery pack ensuring maximized power and energy capabilities without deteriorating the performance as well as safety of energy storage systems. Also the immunity to Electromagnetic Interference (EMI) is necessary for light-emitting diodes (LEDs), high power electronic devices, and high performance energy storage systems. For these, thermoplastic polymers like polyphenylene sulfide (PPS) [3,4], Polysulfone (PSF) [5-7], Polyetherimide (PEI) [8-10], and Polyether ether ketone (PEEK) [11-14] have been developed for improved thermal and electrical conductivities, low coefficient of thermal expansion, inherent flame retardancy, higher mechanical strength, superior chemical resistance, and dimensional stability [15]. However, these polymers exhibit mediocre adhesion properties to other materials (e.g. metals and

ceramics) and do not show desired thermal and electrical properties for the effective heat dissipation and EMI shielding. To address these challenges, the idea of incorporating mechanically strong and conductive carbon nanotubes (CNTs) or graphene as fillers inside of such polymers have been researched and advanced for decades [16–20]. However, using of CNTs or graphene as functional fillers in structural nanocomposite is still expensive. Furthermore, it also requires better dispersion of CNT/graphene in the polymer matrix and effective percolation control for desired electrical and/or thermal conductivities formed during large scale manufacturing processes.

Here we present a multifunctional thin primer film made from the ultrathin CNT network and CNT/epoxy nanocomposite. Our approach for creating this multilayered thin nanocomposite film is as follows. First, by combining CNTs of two different length/diameter aspect ratios (30,000 SWNTs and 200 MWNTs) we achieved significantly enhanced percolation and better dispersion of CNT networks inside of epoxy with a very low CNT concentration (0.05–0.2 wt%) leading to 2–3 orders of magnitude higher electrical and thermal conductivities. This CNT-epoxy film also provides excellent adhesion between the polymer substrate and

^{*} Corresponding author.

E-mail address: jungy@coe.neu.edu (Y.J. Jung).

¹ Authors equally contributed.

thin metal layer, which can be an ideal primer film for a variety of hybrid materials systems. Then a unique convective coating process was developed to assemble very large-scale ultrathin (20-30 nm) and highdensity SWNT films on the surface of hydrophobic CNT/epoxy composite films. SWNT film formed by this approach shows high electrical conductivity $(8.38 \times 10^4 \text{ S/m})$ with only 20–30 nm of thickness, and its electrical conductivity can be further improved by 281% (3.20 \times 10⁵ S/ m) through additional multi-layer coating. This multilayered film of SWNTs networks and CNT/epoxy show high EMI shielding effectiveness (SE) of 24.04 dB (averaged value) in the range of 8.2–12.4 GHz (X-band) and tunable peak EMI SE of 32.54 dB with different wt.% of CNTs in the sandwiched structures. This multilayered nanocomposite can be used for multifunctional adhesive primer film between polymer and metal layer and structurally integrated electrical applications [21] such as electrostatic dissipation, electrostatic painting, and EMI-shielding equipment, and also for various sensing device [22,23] and deicing/thermal management [24,25].

2. Material and methods

Long SWNTs CVD growth. The single-wall carbon nanotube (SWNT, aspect ratio 30,000) was used to enhance the electrical conductivity in CNT/epoxy composite film. The single-wall carbon nanotube was synthesized by a thermal CVD process using anhydrous ethanol (Sigma-Aldrich, 99.95%). Using cobalt catalyst on the oxidized aluminum thin film as prepared growth substrate, the substrates were placed in the quartz tube and heated to 850 °C under a 150 sccm gas flow of 5% hydrogen balanced with argon. 5% hydrogen balanced with argon gas goes through ethanol bubbler and reacts with catalysts for an hour to achieve 30,000 aspect ratio. This long SWNTs are mixed with the short MWNTs to achieve percolation enhanced nanocomposite.

CNT/epoxy composite film. Multi-wall carbon nanotube (MWNT, aspect ratio 200, SES Research) and single-wall carbon nanotube were mixed in a ratio of 1:1 to achieve the enhanced percolation. SPI-Pon 812 epoxy solution was made by mixing SPI-Pon 812 monomer (SPI Supplies), the curing agent Dodecenylsuccinic anhydride (DDSA, SPI Supplies), and the hardener Nadic methyl anhydride (NMA, SPI Supplies) in a ratio of 13:8:7. Then, the mixture of CNT was dispersed into the SPI-Pon 812 resin solution to obtain 0.05 wt%, 0.1 wt% and 0.2 wt% CNT/epoxy composite dispersions. After adding 3 wt% of the accelerator N-Benzyldimethylamine (BDMA, SPI Supplies), the CNT/epoxy dispersions were spin-coated on PPS and baked at 150 °C for 3 h to get 50 µm composite films. This mixed CNT/epoxy film showed better performance than the MWNT/epoxy film.

Thin CNT film assembly using CNT-Alcohol solution. In order to assemble thin CNT film on the super hydrophobic substrate without any substrate treatment, the coating method using CNT-Alcohol solution was developed. IPA and DI water were mixed in a ratio of 3:7 (v/v). Then the IPA/DI water mixture was further mixed with CNT solution (0.05 wt%, Brewer Science) in a ratio of 2:3 (v/v) on the PPS (INITZ) or CNT/Epoxy substrate. The substrate was preheated at 65 °C on a hotplate for 5 min. When the substrates meets desired temperature, CNT solution and IPA/DI water mixture was poured onto the substrate to cover the whole surface. The substrate and CNT-IPA/DI water mixture solution were baked at 65 °C on a hotplate until completely dried. This method results in the ultrathin CNT network (25 nm thickness) with very high coverage.

CNT/Epoxy and CNT film sandwich structure (CEC structure). CEC structure was considered in order to fabricate the multifunctional primer film. The 0.1 wt% CNT/epoxy composite film was spin coated on the PPS substrate. Then 0, 1, 5 and 10 layers of CNT films were coated respectively on the as-fabricated CNT/epoxy composite film with the method described above. Another 0.1 wt% CNT/epoxy composite film was spin coated atop. This CEC structure is the final structure of a multifunctional primer film.

3. Calculation and characterization

The electrical resistance was measured by the four-point probe method using Keithley 2460 Source Meter. The sheet resistance (R_s) was calculated by using the equation, $R_s = \left(\frac{\pi}{\ln(2)} \frac{\Delta V}{I}\right)$, and the electrical conductivity (σ) was calculated with sheet resistance and geometric correction factors [26,27].

The thermal conductivity of CNT/epoxy composite film was measured by a self-heating 3ω technique. To reduce the radial heat losses through gas conversion, all the measurements (resistance, temperature, and 3ω signals) were performed under high vacuum (p < 10-5 Torr) on a Janis Research ST-500 cryogenic probe station.

Before surface roughness and adhesion tests, 100 nm Aluminum was deposited on the surface by magnetron-sputtering (PerkinElmer 2400). The surface roughness map was obtained using an optical surface profiler (Zygo Newview 6000). The tape adhesion test was performed according to ASTM D3359. Six parallel cuts were made for 2 mm apart with a 20 mm length, followed by another six parallel cuts in the perpendicular direction to create a grid area. The film was then brushed lightly to remove any detached flakes or ribbons of coatings. Then the scotch tape was placed over the grid and rubbed firmly with an eraser for 90 s. After applying for 90 s rubbing, hold the free end (the end of the attached tape) and pull the tape rapidly as close as possible to 180° to remove the tape. The grid area was then inspected for the removal of coating from a substrate, and the adhesion was rated in accordance with the scale.

The contact angles were measured on the PPS substrate using Phoenix 150 Contact angle measurement system. The scanning electron microscopy (SEM) images were taken on a SUPRA 25 FESEM.

EMI shielding effectiveness measurements were performed using a coaxial test cell (APC-7 connector, frequency up to 18 GHz) in conjunction with an Agilent E8364A vector network analyzer according to ASTM ES7-83, which is capable of measuring incident, transmitted, and reflected powers. The EMI SE measurements were carried out between 8.2 GHz and 12.4 GHz (X Band) and SE is calculated by comparing the difference in attenuation of a reference into our CNT/Epoxy composite sample. The intermediate frequency bandwidth was set as 1 kHz and 1601 points were collected for each specimen during the measurement. The composite films were peeled off the PPS substrate, cut into 11 mm in diameters, and placed in the specimen holder which were connected through a pair of 50 Ω double-shield Agilent E8364A coaxial cables to separate VNA ports. The scattering parameters (S11 and S21) of the CNT/epoxy composites in the X-Band were obtained for the calculation of EMI SE. The overall EMI SE of the composites was determined from equation (1) below in decibel (dB) [28].

EMI SE =
$$10 \log \left(\frac{P_T}{P_I} \right) = 20 \log \left(\frac{E_T}{E_I} \right)$$
 (1)

where P_I and E_I are incident power and field strength and P_T and E_T are transmitted power and field strength, respectively.

4. Results and discussion

4.1. Fabrication of percolation enhanced CNT/polymer nanocomposite film with extremely low CNT concentration

According to the percolation theory, CNTs with a higher L/D (length/diameter) aspect ratio will form a better conductive CNT network inside of polymer while limits the effective dispersion of CNTs [29]. On the other hand, CNTs with a lower L/D aspect ratio show the enhanced mobility of CNTs during the dispersion inside polymers but it results in lower percolation of CNT network [30]. In order to achieve both higher percolation and effective dispersion of CNTs within the polymer matrix, we mixed two very different L/D aspect ratios of CNTs

(30,000 SWNTs and 200 MWNTs) in the polymer matrix [31–33] (Fig. 1a). Epoxy, commonly used for the adhesive layer for their good wettability to other polymers as well as CNTs, has been used for the CNT-nanocomposite film. The mixture of short MWNTs and long SWNTs (1:1 w/w) and SPI-Pon 812 epoxy monomers were mixed together and well-dispersed by sonication. Then the CNT/Epoxy mixture was spin-coated on the PPS substrate followed by polymerization at 150 °C to obtain a 50 μ m CNT/epoxy composite film on the PPS.

Fig. 1b demonstrates highly enhanced electrical percolation of CNT network within the epoxy matrix when CNTs with two very different L/ D aspect ratios was used. Even with the extremely low loadings of mixed CNTs in the epoxy matrix – 0.05 wt%, 0.1 wt%, and 0.2 wt%, the composite films show remarkably higher electrical conductivity than CNT/ Epoxy composite films made with short MWNTs only. We found that the percolation threshold is between 0.05 wt% and 0.1 wt% of CNTs (Fig. 1b). The CNT/epoxy composite with the mixture of long SWNTs and short MWNTs shows 30 times higher electrical conductivity $(1.29 \times 10^{-2} \,\text{S/m})$ than the CNT/epoxy composite film only with short MWNTs $(4.32 \times 10^{-4} \text{ S/m})$ at 0.05 wt% CNTs. Supplemental Fig. S1 shows the electrical conductivity of long SWNTs and short MWNTs with polymer composite respectively. With increasing concentration of the CNTs to 0.2 wt%, the mixed CNT/Epoxy composite shows exceptionally increased electrical conductivity of 0.471 S/m, which is 3 order of magnitude higher than that of the MWNTs/epoxy composite film $(4.49 \times 10^{-4} \text{ S/m})$ and other reported results [34–36]. Using 3- Ω method, we also characterized thermal conductivities of our percolation enhanced CNT-epoxy film. A thermal conductivity of 1.9 W/m·K was measured with mixed 0.1 wt% CNTs-epoxy film which is eight times higher than thermal conductivities of other reported CNT/epoxy composites with similar CNT concentration [29,37,38].

To use as a primer film for thin metal layer coating on polymer substrate, the surface roughness and adhesion strength of CNT/Epoxy composite films were investigated. The characteristics of surface roughness of CNT/epoxy composite films with various CNT

concentrations were measured by the optical surface profiler (Fig. 1c). The averages roughness for 0.05 wt%, 0.1 wt%, and 0.2 wt% CNT/epoxy composite films are 46 nm, 105 nm and 313 nm, respectively. As the concentration of the CNT increases, the surface roughness also increases. The averaged roughness of 0.05 wt% CNT/epoxy composite film was 46 nm, which is lower than that of PPS (56 nm) and PPS/TPU (62 nm). The fabrication process and the properties for CNT/TPU composites are available in Supplemental Fig. S2. To characterize the light reflectance and adhesion strength, 100 nm thickness of Al film was deposited on the CNT/epoxy composite using a sputtering coating method. Fig. 1d shows the normalized reflectance change after Al deposition. 0.05 wt%, 0.1 wt %, and 0.2 wt% CNT/epoxy composite films show increased reflectance of 159.3%, 149.9%, and 140.5% compared to the reflectance of a bare PPS/Al, respectively. Though the 0.1 wt% and 0.2 wt% CNT/epoxy composite films have higher surface roughness (shown in Fig. 1c) than that of PPS substrate, all CNT-epoxy films showed higher values of normalized reflectance change than that of bare PPS substrate. We speculate that this is due to highly enhanced adhesion between Al and CNT-epoxy films leading to uniform coating of Al thin film. In CNT/ epoxy structures, normalized reflectance were slightly decreased by increasing CNT wt.%, indicating that reflection loss was increased with increasing CNT concentration [39]. To evaluate the adhesion property of Al thin film on the CNT-epoxy composite substrate, the standard tape adhesion test (ASTM D3359) was performed on 0.1 wt% CNT/epoxy composite film and the bare PPS substrates. The bare PPS sample and Al shows 0B of adhesion classification (Fig. 1e (bottom)), showing that all Al films were removed after the adhesion test. However for 0.1 wt% CNT-epoxy composite film, most of the Al film was intact after the adhesion test (0.1 wt/% CNT/epoxy primer), as referred to classification 5B, indicating the satisfactory wettability for a primer film between PPS substrate and the Al layer (shown in Fig. 1e (top)). We speculate that the CNT/epoxy composite film has higher surface energy than PPS, which brings higher adhesive force to both PPS substrate and the Al layer. Also, the CNT/epoxy composite film may have a larger number of hydroxyl

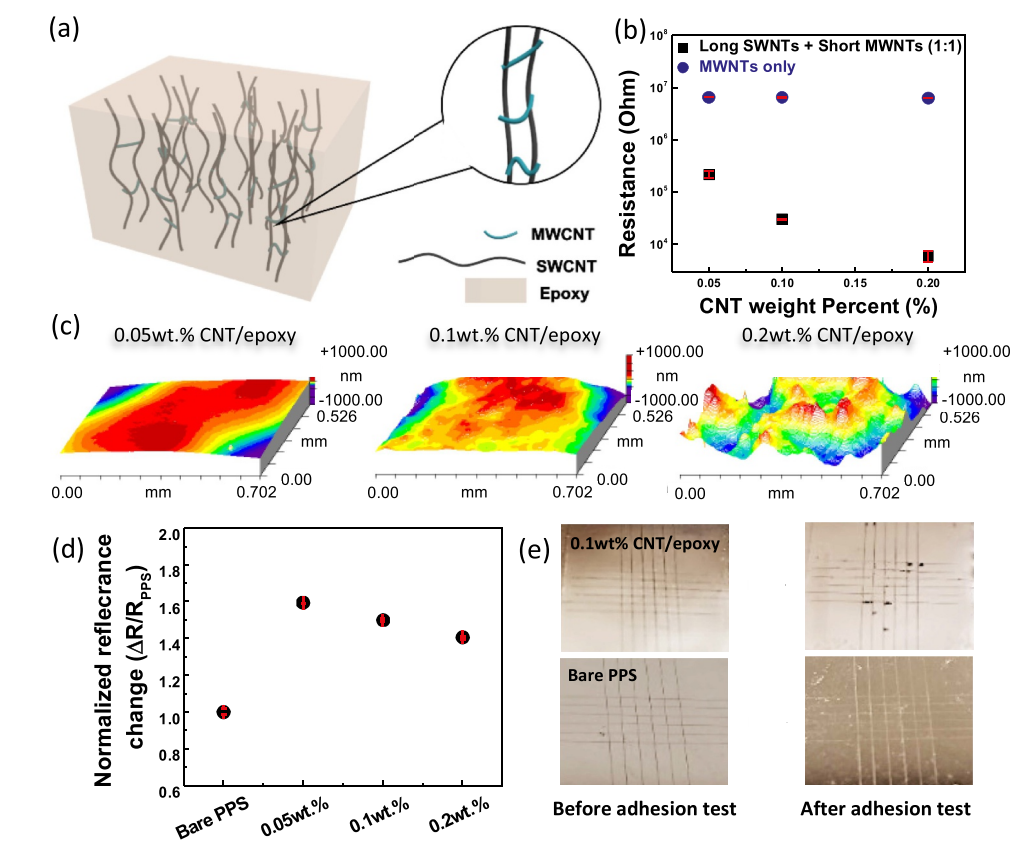


Fig. 1. (a) Schematic of CNT/Epoxy composite primer film, showing percolation of long SWNTs and short MWNTs. (b) Electrical conductivity changes in log scale along the CNT weight percentage (0.05 wt%, 0.1 wt%, and 0.2 wt%) in CNT/Epoxy composite layer, with mixed CNTs (SWNTs + MWNTs) and with only MWNTs. (c) Surface roughness map of CNT/epoxy composite film: from the left 0.05 wt% CNT/Epoxy, 0.1 wt% CNT/ Epoxy, and 0.2 wt% CNT/Epoxy. (d) Normalized reflectance data of bare PPS/Al, 0.05 wt%, 0.1 wt%, and 0.2 wt% CNT/Epoxy composite film/Al. (e) Optical images of adhesion test of bare PPS/0.1 wt% CNT/ Epoxy composite primer film/Al (top) and PPS/Al (bottom): before (Left) and after (Right).

groups which have a strong attraction to the metal layers to form bonds [40,41].

4.2. Assembly of ultrathin CNTs on the CNT-epoxy nanocomposite film

Conventional CNT assembly methods, particularly on hydrophobic polymer surfaces, require pre-surface treatment in order to reduce hydrophobicity and decrease contact angle between CNT solution and substrates [42]. For example, oxygen plasma, UV plasma, low-pressure cold gas plasma (Microwave/RF), electrical (corona discharge), and flame plasma were used to increase surface energy and improve wetting [43]. However, superhydrophobic substrates like PPS show very high contact angle after the pre-surface treatment which indicates that conventional CNT assembly methods cannot be applied to the superhydrophobic substrates (Supplemental Fig. S3).

In order to further increase electrical conductivity and related EMI shielding effectiveness of the primer film, ultrathin CNT film (20-30 nm thickness) was coated on CNT-epoxy composite film by employing our newly developed assembly process, called convective coating of CNT film with CNT-Alcohol solution. Using the convective nature within CNT-DI water and alcohol solution, we could achieve a very low contact angle with highly stable interfacial balance between solution and substrates of polymers (including superhydrophobic PPS) without any surface pretreatment. Supplemental Figs. S4-S6 show a detailed CNT coating process and related mechanism with and without IPA in the CNT solution. To assemble ultrathin CNT film on the surface of CNT-epoxy composite, this convective assembly process was directly applied at $65\,^{\circ}\text{C}$ until all IPA and DI water evaporate. If the CNT solution does not contain IPA, the CNT solution recedes during the coating process, resulting in very thick and non-uniform coating of CNT film due to its high contact angle (Supplemental Fig. S6). However, the CNT-IPA/DI water mixture solution enables an extremely low contact angle below 10° and maintains a highly stable liquid and solid interface between solution and substrates (PPS or CNT/Epoxy composite film) leading to the formation of ultrathin (20-30 nm thickness) and uniform CNT film (Fig. 2a and b).

The electrical conductivity of assembled CNT thin film was measured using a four-point measurement method. Results show that our thin CNT

film has high electrical conductivity of 8.38×10^4 S/m. We could further increase the electrical conductivity up to 3.20×10^5 S/m by performing multiple processes of convective coating of CNTs which add more CNT layers on the film (Fig. 2c). When IPA and DI water are mixed into the CNT solution, the entropy of mixing occurs and disrupts the hydrogen bonding network in the mixture. The mixing entropy by adding IPA and DI water into the CNT solution makes the mixed solution keep mixing/ moving and makes CNTs move toward the boundary between solid and liquid [44]. This phenomenon makes CNT concentration of the center part of film slightly higher than the edge part of film (Fig. 2d) at the first layer. However, this issue could be fixed simply by the multilayered coating method. The ultrathin CNT film has only around 125 nm thickness for five multilayers but achieves exceptional electrical conductivity throughout the entire sample area. Supplemental Fig. S7 shows other properties of this ultrathin CNT film such as reflectance, adhesion, and roughness.

4.3. Sandwiched structure of CNT-epoxy nanocomposite and thin CNT film

The CNT-Epoxy nanocomposite film and CNT layers sandwiched structure (CEC sandwich structure) was developed to make a primer film for both higher conductivities and EMI shielding effectiveness. Fig. 3a-d (left) are schematics of CEC sandwich structures we created where ultrathin CNT films are placed between the two CNT-Epoxy composite films with the different CNT layers (0 layer, 1 layer, 5 layers, and 10 layers) and concentration of CNT (0.05 wt%, 0.1 wt%, and 0.2 wt%) in the epoxy film. The thickness of CEC sandwich structures (with or without CNT thin film) is about 100 µm. The electrical conductivity (Fig. 3e) was measured by the four-probe measurement method. CEC sandwich structure (0.1 wt% CNT inside of epoxy) with 10 layers of CNT film shows about 45 times higher electrical conductivity (3.38 S/m) than that of 0.1 wt% sandwiched structure of CNT-epoxy nanocomposite film without CNT thin film (7.54E-2 S/m). As shown in Fig. 3f, the CEC sandwich structures also show improved normalized reflectance of 156% for all conditions (0 layer, 1 layer, 5 layer, and 10 layer) compared to the bare PPS/Al. The reflectance of CEC sandwich structure is also greater than 0.1 wt% of CNT/epoxy composite film (149.9%, thickness

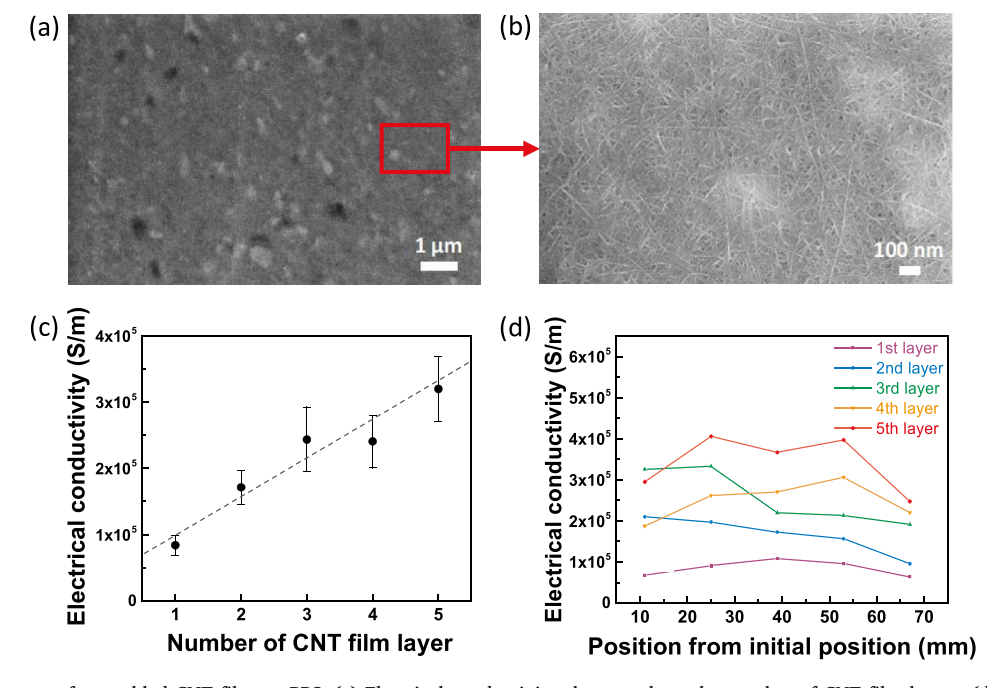


Fig. 2. (a), (b) SEM images of assembled CNT film on PPS. (c) Electrical conductivity changes along the number of CNT film layers. (d) Electrical conductivity changes throughout the CNT film's horizontal positions.

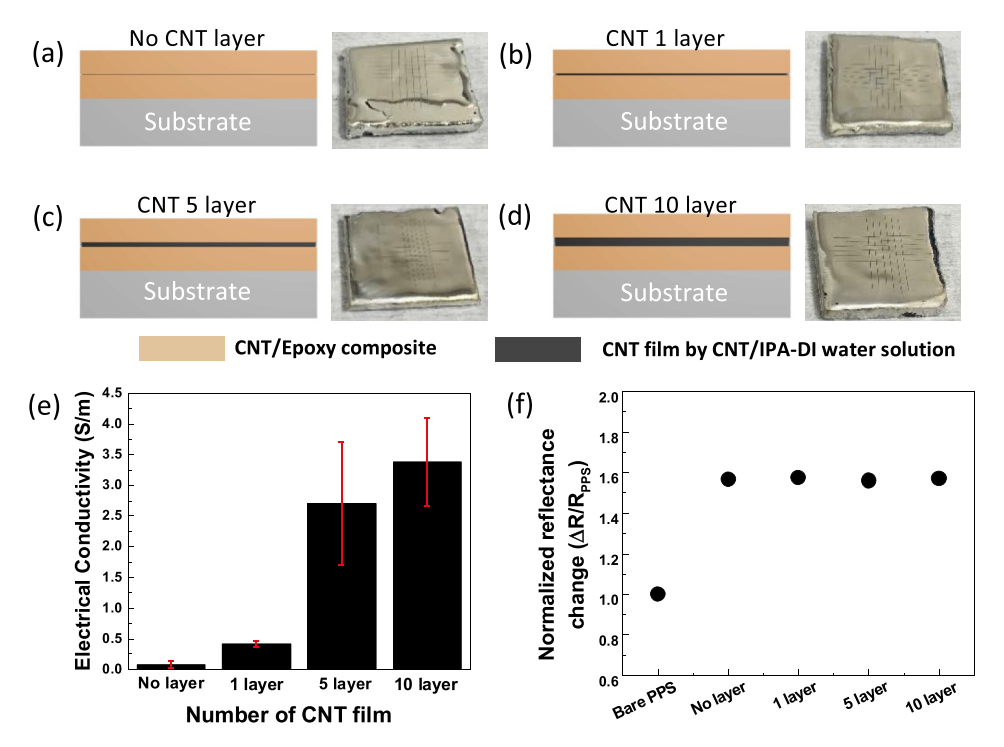


Fig. 3. (a)–(d) (Left) schematic of the sandwich structure of 0.1 wt% CNT/Epoxy composite. (right) optical images after adhesion test (100 nm of aluminum deposited on top) with: (a) no CNT film. (b) 1 layer of CNT film. (c) 5 layer of CNT film. (d) 10 layer of CNT film. (e) Electrical conductivity of the CEC sandwich structure with various CNT layers. (f) Normalized reflectance data of the CEC sandwich structure with various CNT layers.

 $50\,\mu m),$ which indicates that multiple spin coating process of CNT/epoxy composite film (in our case, two times) does not affect reflectance. For the surface roughness, sandwiched structure does not make the surface rougher, instead makes the surface even smoother than one time of spin coating of CNT/Epoxy composite film. As shown in Fig. 3a–d

(right), the CEC sandwich structure shows excellent adhesion with thin Al film (classification of 5B using ASTM D3359), which indicates none of Al film was removed after the adhesion test.

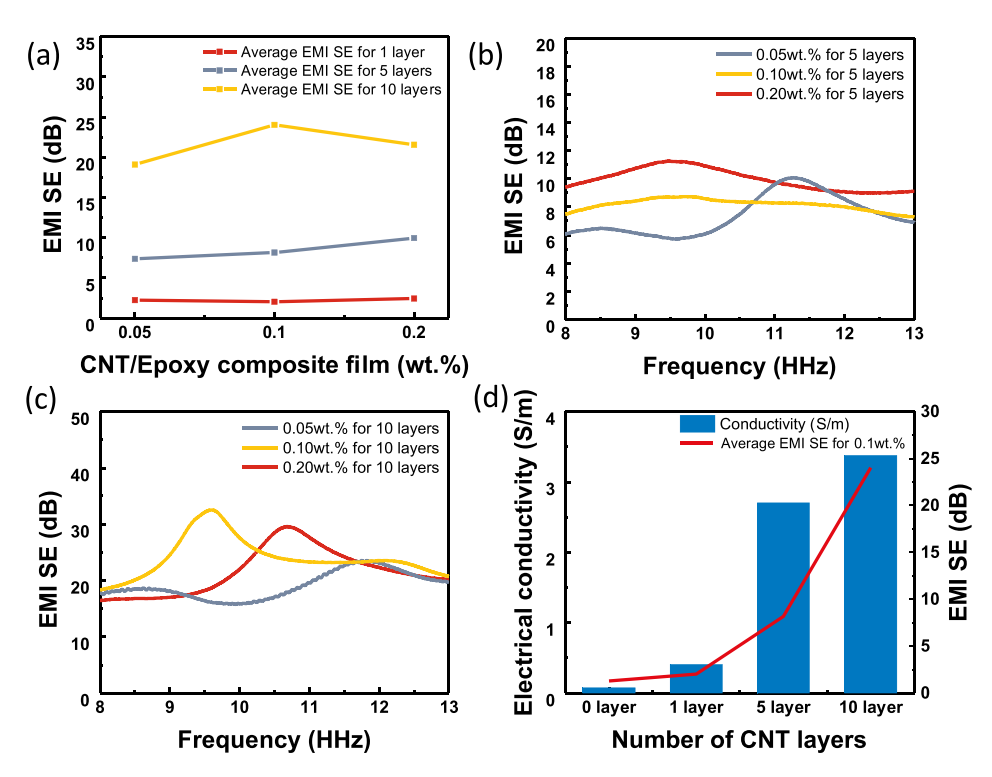


Fig. 4. (a) Averaged EMI-shielding effectiveness of sandwich structures as function of concentration of 0.05 wt%, 0.1 wt%, and 0.2 wt%. (b)–(c) EMI-shielding effectiveness of sandwich structures according to different concentration of CNTs for: (b) 5 layer CNT films and (c) 10 layer CNT films. (d) Electrical conductivity and EMI SE as a function of the number of CNT layers for 0.1 wt%.

4.4. EMI shielding effectiveness of sandwiched structure of CNT-epoxy composite and ultrathin CNT film

The EMI shielding effectiveness is the measurement of attenuation from incident radiation when electromagnetic waves propagate through a shielding material. Shielding material should have good properties of maximizing attenuation of the electromagnetic wave by absorption or reflection with lower transmission component. The sandwich architectures of CNT-epoxy composite and ultrathin CNT film were tested at frequency range of 8.2 GHz–12.4 GHz (X band) which is widely used for radar and satellite communication system in the military applications [45].

Fig. 4a shows EMI shielding effectiveness of the sandwich structures of CNT-epoxy composite and ultrathin CNT film as a function of CNT/ Epoxy composite (wt.%). The values of EMI SE were 2.23 dB, 8.49 dB, and 21.56 dB on the average of wt.% for 1 layer, 5 layers, and 10 layers of CNT film, respectively. With increasing CNT/Epoxy composite wt.%, EMI SE tended to slightly increase for each layer but within 10% range of SE. However, the average value of shielding effectiveness for each layer was surprisingly increased by 280% from 1 layer to 5 layers and by 153% from 5 layers to 10 layers. The EMI shielding effectiveness for 5 and 10 layers of ultrathin CNT films within CEC structures are average of 10 dB and 24 dB (0.1 wt% CNT/Epoxy composite film) in the entire X band range respectively which is 10-16 times higher shielding effectiveness than that of the CNT-epoxy nanocomposite film. Moreover this high EMI shielding effectiveness couldn't be achieved with even 15 wt %. of SWNTs in millimeter thickness of other CNT-epoxy nanocomposite [32,35]. Increasing the number of CNT film layers in the sandwich architecture showed much enhanced EMI SE compared to the increase in wt.% of CNT/Epoxy composite. For the fixed number of CNT film layers, the values of EMI SE in X band were represented in Fig. 4b and c. In case of 5 layers of CNT film EMI SE increased by 2 dB in frequency range at 8 GHz-10.5 GHz by increasing wt.% of CNTs. The maximum EMI SE values are different from the amount of CNT's wt.%. For 0.1 wt% with 10 layers EMI SE shows a peak value of 32.54 dB at 9.59 GHz and for 0.2 wt% EMI SE shows a peak of 29.57 dB at 10.68 GHz. By increasing 0.1 wt% of CNTs in the CEC structure, the peak point of EMI SE was shifted by about 1 GHz from 9.59 GHz. EMI SE values can be tunable by controlling concentration of CNTs in sandwich structures for 10 layers of CNT film. And it was also observed that the increase of EMI shielding effectiveness with increasing frequency is due to decrease in film depth of the sandwich structure with increasing frequency [46]. The observed high EMI SE of sandwich architectures with increasing CNT layers can be attributed to their high electrical conductivity. Fig. 4d show the relationship between electrical conductivity and EMI SE as a function of the number of CNT layers for 0.1 wt%. There is a strong correlation of r = 0.88 between them represented in Supplemental Fig. S8. EMI shielding effectiveness of 100 µm thickness of CNT-Epoxy nanocomposite film with 0.05 wt%, 0.1 wt%, and 0.2 wt% CNTs is presented in Supplemental Fig. S9a. All CNT-epoxy nanocomposite films show EMI shielding effectiveness around 1.5 dB ranging from 8.2 GHz to 12.4 GHz, X-band. This is certainly remarkable result as a better or similar shielding effectiveness was achieved with 100 µm thickness of CNT-epoxy nanocomposite film compared to other reported CNT-epoxy nanocomposites with millimeters thickness [32,35,47,48]. EMI shielding effectiveness with fixed wt.% of CNT/Epoxy was further increased by employing the CEC sandwich structure with additional CNT film layers (Supplemental Figs. S9b-d).

5. Conclusion

In summary we present a multifunctional primer film made from carbon nanotube-epoxy nanocomposite and ultrathin CNT films. Significantly enhanced percolation and better dispersion of CNT networks inside of epoxy was achieved by combining CNTs of two different length/diameter aspect ratios (30,000 SWNTs and 200 MWNTs) with a

very low CNT concentration (0.05–0.2 wt%). We also deposit SWNTs into ultrathin (20–50 nm) and high-density films on the hydrophobic surface CNT/epoxy composite films by developing a unique convective CNT assembly process. This strategy could be applied multiple times to create multilayered sandwich structured carbon nanotube-epoxy nanocomposite and ultrathin CNT films. This multilayered primer film demonstrates excellent adhesion strength to other polymers and metal layers, high optical reflectance, significantly improved electrical conductivity (3.38 S/m), excellent EMI shielding effectiveness with tunable structures in the X-band range for only 100 μm of thickness. The strategy and result reported here allow us to design multifunctional primer thin films that can be also used for hybrid thermal management devices, EMI shielding film and structurally integrated sensors.

Acknowledgement

This work was supported by the Industrial Strategic Technology Development Program (10050481, Development of High Stiffness and Thermal Resistant Materials for High Performance Automotive Lighting System) funded by the Ministry of Trade, Industry and Energy (MOTIE) of Korea. YJJ also acknowledges the funding from National Science Foundation, PFI program (award number: 1701043). We thank Ji Hao and Yongheum Choi for technical help.

Appendix A. Supplementary data

Supplementary data to this article can be found online at https://doi.org/10.1016/j.compositesb.2019.107107.

References

- Joshi M, Chatterjee U. Polymer nanocomposite: an advanced material for aerospace applications. In: Advanced composite materials for aerospace engineering; 2016. p. 241–64.
- [2] Lyu M, Choi T. Research trends in polymer materials for use in lightweight vehicles. Int J Precis Eng Manuf 2015;16(1):213–20.
- [3] Platt DK. Engineering and high performance plastics market report: a Rapra market report. iSmithers Rapra Publishing; 2003.
- [4] Jiang Z, Hornsby P, McCool R, Murphy A. Mechanical and thermal properties of polyphenylene sulfide/multiwalled carbon nanotube composites. J Appl Polym Sci 2012;123(5):2676–83.
- [5] Podgórski M, Wang C, Yuan Y, Konetski D, Smalyukh I, Bowman C. Pristine polysulfone networks as a class of polysulfide-derived high-performance functional materials. Chem Mater 2016;28(14):5102–9.
- [6] Chen X, Tang B, Luo J, Wan Y. Towards high-performance polysulfone membrane: the role of PSF-b-PEG copolymer additive. Microporous Mesoporous Mater 2017; 241:355–65.
- [7] Yue W, Li H, Xiang T, Qin H, Sun S, Zhao C. Grafting of zwitterion from polysulfone membrane via surface-initiated ATRP with enhanced antifouling property and biocompatibility. J Membr Sci 2013;446:79–91.
- [8] Stegelmann M, Lucas P, Modler N. Design and extrusion of high-performance polyetherimide pipes with variable wall thickness for aircrafts. In AIP conference Proceedings2019. p. 070008.
- [9] Pitchan M, Bhowmik S, Balachandran M, Abraham M. Effect of surface functionalization on mechanical properties and decomposition kinetics of high performance polyetherimide/MWCNT nano composites. Compos Appl Sci Manuf 2016;90:147–60.
- [10] Guo D, Khan A, Liu T, Zhou Z, Liu G. Sub-10 nm domains in high-performance polyetherimides. Polym Chem 2019;10(3):379–85.
- [11] Garcia-Gonzalez D, Rusinek A, Jankowiak T, Arias A. Mechanical impact behavior of polyether-ether-ketone (PEEK). Compos Struct 2015;124:88–99.
- [12] Rinaldi M, Puglia D, Dominici F, Cherubini V, Torre L, Nanni F. Melt processing and mechanical property characterization of high-performance poly (ether ether ketone)—carbon nanotube composite. Polym Int 2017;66(12):1731–6.
- [13] Kurtz S, Devine J. PEEK biomaterials in trauma, orthopedic, and spinal implants. Biomaterials 2007;28(32):4845–69.
- [14] Rival G, Paulmier T, Dantras E. Effect of electronic irradiations on electrical properties of a high-performance space-used thermoplastic polymer. In: Proceedings of international symposium on materials in space environment (ISMSE). Conference. Conference; 2018.
- [15] Queisser J, Geprägs M, Bluhm R. Trends in automotive headlamps. Kunstst Plast Eur 2002;92(3):32–4.
- [16] Shtein M, Nadiv R, Buzaglo M, Kahil K, Regev O. Thermally conductive graphene-polymer composites: size, percolation, and synergy effects. Chem Mater 2015;27 (6):2100–6.

- [17] Nadiv R, Shtein M, Buzaglo M, Peretz-Damari S, Kovalchuk A, Wang T, et al. Graphene nanoribbon–Polymer composites: the critical role of edge functionalization. Carbon 2016;99:444–50.
- [18] Nadiv R, Shachar G, Peretz-Damari S, Varenik M, Levy I, Buzaglo M, et al. Performance of nano-carbon loaded polymer composites: dimensionality matters. Carbon 2018;126:410–8.
- [19] Chen J, Yan L, Song W, Xu D. Interfacial characteristics of carbon nanotubepolymer composites: a review. Compos Appl Sci Manuf 2018;114:149–69.
- [20] Wu H, Jia L, Yan D, Gao J, Zhang X, Ren P, et al. Simultaneously improved electromagnetic interference shielding and mechanical performance of segregated carbon nanotube/polypropylene composite via solid phase molding. Compos Sci Technol 2018;156:87–94.
- [21] Ramasubramaniam R, Chen J, Liu H. Homogeneous carbon nanotube/polymer composites for electrical applications. Appl Phys Lett 2003;83(14):2928–30.
- [22] Li L, Yang Z, Gao H, Zhang H, Ren J, Sun X, et al. Vertically aligned and penetrated carbon nanotube/polymer composite film and promising electronic applications. Adv Mater. 2011;23(32):3730–5.
- [23] Philip B, Abraham J, Chandrasekhar A, Varadan V. Carbon nanotube/PMMA composite thin films for gas-sensing applications. Smart Mater Struct 2003;12(6): 935
- [24] Chu H, Zhang Z, Liu Y, Leng J. Self-heating fiber reinforced polymer composite using meso/macropore carbon nanotube paper and its application in deicing. Carbon 2014;66:154–63.
- [25] Huang H, Liu C, Wu Y, Fan S. Aligned carbon nanotube composite films for thermal management. Adv Mater 2005;17(13):1652–6.
- [26] Topsoe H. Geometric factors in four point resistivity measurement. Bulletin 1968; 472(13):63.
- [27] Smits F. Measurement of sheet resistivities with the four-point probe. Bell Syst Tech J 1958;47(4):711–8.
- [28] Ozen M, Sancak E, Beyit A, Usta I, Akalin M. Investigation of electromagnetic shielding properties of needle-punched nonwoven fabrics with stainless steel and polyester fiber. Textil Res J 2013;83(8):849–58.
- [29] Bryning M, Milkie D, Islam M, Kikkawa J, Yodh A. Thermal conductivity and interfacial resistance in single-wall carbon nanotube epoxy composites. Appl Phys Lett 2005;87(16):161909.
- [30] Martin C, Sandler J, Shaffer M, Schwarz M, Bauhofer W, Schulte K, et al. Formation of percolating networks in multi-wall carbon-nanotube-epoxy composites. Compos Sci Technol 2004;64(15):2309–16.
- [31] Li N, Huang Y, Du F, He X, Lin X, Gao H, et al. Electromagnetic interference (EMI) shielding of single-walled carbon nanotube epoxy composites. Nano Lett 2006;6 (6):1141–5.
- [32] Huang Y, Li N, Ma Y, Du F, Li F, He X, et al. The influence of single-walled carbon nanotube structure on the electromagnetic interference shielding efficiency of its epoxy composites. Carbon 2007;45(8):1614–21.

- [33] Zeng X, Xu X, Shenai P, Kovalev E, Baudot C, Mathews N, et al. Characteristics of the electrical percolation in carbon nanotubes/polymer nanocomposites. J Phys Chem C 2011;115(44):21685–90.
- [34] Gojny F, Wichmann M, Fiedler B, Kinloch I, Bauhofer W, Windle A, et al. Evaluation and identification of electrical and thermal conduction mechanisms in carbon nanotube/epoxy composites. Polymer 2006;47(6):2036–45.
- [35] Chen Y, Zhang H, Yang Y, Wang M, Cao A, Yu Z. High-performance epoxy nanocomposites reinforced with three-dimensional carbon nanotube sponge for electromagnetic interference shielding. Adv Funct Mater 2016;26(3):447–55.
- [36] Guadagno L, Vietri U, Raimondo M, Vertuccio L, Barra G, De Vivo B, et al. Correlation between electrical conductivity and manufacturing processes of nanofilled carbon fiber reinforced composites. Compos B Eng 2015;80:7–14.
- [37] Moisala A, Li Q, Kinloch I, Windle A. Thermal and electrical conductivity of singleand multi-walled carbon nanotube-epoxy composites. Compos Sci Technol 2006;66 (10):1285–8.
- [38] Biercuk M, Llaguno M, Radosavljevic M, Hyun J, Johnson A, Fischer J. Carbon nanotube composites for thermal management. Appl Phys Lett 2002;80(15): 2767–9
- [39] Gui X, Wang K, Cao A, Wei J, Lv R, Kang F, et al. Selective microwave absorption of iron-rich carbon nanotube composites. J Nanosci Nanotechnol 2010;10(3): 1808–13
- [40] Ismaili NA, Chenouni D, Lakhliai Z, El-Kettani ME-C, Morvan B, Izbicki J-l. Determination of epoxy film parameters in a three-layer metal/adhesive/metal structure. IEEE Trans Ultrason Ferroelectr Freq Control 2009;56(9):1955–9.
- [41] Andrews E, King N. Adhesion of epoxy resins to metals. J Mater Sci 1976;11(11): 2004–14.
- [42] Tan SH, Nguyen NT, Chua YC, Kang TG. Oxygen plasma treatment for reducing hydrophobicity of a sealed polydimethylsiloxane microchannel. Biomicrofluidics 2010;4(3):032204.
- [43] Sabreen S. Surface wetting & pretreatment methods. The Sabreen Group, Inc.; 1991. p. 1–2.
- [44] Lam R, Smith J, Saykally R. Communication: hydrogen bonding interactions in water-alcohol mixtures from X-ray absorption spectroscopy. J Chem Phys 2016; 144:191103
- [45] NATO. NATO joint civil/military frequency agreement. NJFA); 2014.
- [46] Modak P, Kondawar SB, Nandanwar D. Synthesis and characterization of conducting polyaniline/graphene nanocomposites for electromagnetic interference shielding. Procedia Mater Sci 2015;10:588–94.
- [47] Jana P, Mallick A, De S. Effects of sample thickness and fiber aspect ratio on EMI shielding effectiveness of carbon fiber filled polychloroprene composites in the Xband frequency range. IEEE Trans Electromagn Compat 1992;34(4):478–81.
- [48] Yan D, Pang H, Li B, Vajtai R, Xu L, Ren P, et al. Structured reduced graphene oxide/polymer composites for ultra-efficient electromagnetic interference shielding. Adv Funct Mater 2015;25(4):559–66.